

Electronic Supplementary Information

Real-time imaging of alkaline phosphatase activity of diabetes in mice via a near-infrared fluorescence probe

Wen-Xin Wang,^a Wen-Li Jiang,^a Hong Guo,^a Yongfei Li,^{a,b} and Chun-Yan Li^{*a}

^a Key Laboratory for Green Organic Synthesis and Application of Hunan Province, Key Laboratory of Environmentally Friendly Chemistry and Applications of Ministry of Education, College of Chemistry, Xiangtan University, Xiangtan, 411105, PR China.

^b College of Chemical Engineering, Xiangtan University, Xiangtan, 411105, PR China.

*Corresponding Author. E-mail: lichunyan79@sina.com.

Table of contents

1. Experimental Section	S3
2. Synthesis of probes	S6
3. Spectral data.....	S12
4. Response mechanism	S15
5. Biological assays.....	S19

1. Experimental Section.

Reagents and instruments. 2-Methylquinoline, iodoethane ($\text{CH}_3\text{CH}_2\text{I}$), cyclohexanone, 2-hydroxy-4-methoxybenzaldehyde, phosphorus tribromide (PBr_3), cesium carbonate (Cs_2CO_3) boron tribromide (BBr_3) phosphorus oxychloride (POCl_3) were purchased from Aladdin (Shanghai, China). streptozotocin (STZ), metformin (Metf) were purchased from Sigma-Aldrich (St. Louis, USA). ALP (alkaline phosphatase) was purchased from TaKaRa Biotechnology Corporation (Dalian, China). Unless otherwise stated, all chemicals were purchased from commercial suppliers and used without further purification.

Nuclear magnetic resonance (NMR) spectra were measured on a Bruker Avance II NMR spectrometer (Germany). ^1H , ^{13}C NMR were conducted at 400, 100 MHz, respectively. Mass Spectra (MS) was recorded on a Bruker Autoflex MALDI-TOF mass spectrometer (Germany). HPLC was carried out on a Agilent 1260 LC system with a C18 column (USA). Elemental analysis was obtained on a PerkinElmer 2400 elemental analyzer (USA). The fluorescence spectrum determined by a PerkinElmer LS-55 fluorescence spectrometer (USA). The absorption spectra determined by a PerkinElmer Lambda 25 UV/vis spectrophotometer (USA). Fluorescence imaging of cells were carried out by a Nikon confocal fluorescence microscope (Japan). Fluorescence imaging of mice was performed on an IVIS Lumina XR small animal optical in vivo imaging system (USA).

General procedure for fluorescence measurement. The fluorescence spectra were performed in the following steps. ALP with different activity from 0.05 to 1 U/mL was added into 4 mL of 50 mM Tris-HCl buffer solution (pH 8.0) containing 10 μM QX-P and 1 mM MgCl_2 . The fluorescent spectra were recorded at 37 °C at the emission wavelength ranged

from 730 to 875 nm and the excitation wavelength of 720 nm. The excitation slit and emission slit were both set at 10.0 nm.

Determination of Detection Limit. The detection limit was calculated according to the fluorescence titration. The emission intensity of QX-P in the absence of ALP in Tris-HCl buffer solutions (50 mM, pH 8.0) was calculated three times, and the standard deviation of blank measurements was determined. Three independent duplication measurements of emission intensity were performed in the presence of ALP, and each average value of the intensities was plotted as a concentration of ALP for determining the slope. The detection limit is then calculated with eq 1:

$$\text{detection limit} = 3\sigma/k \quad (1)$$

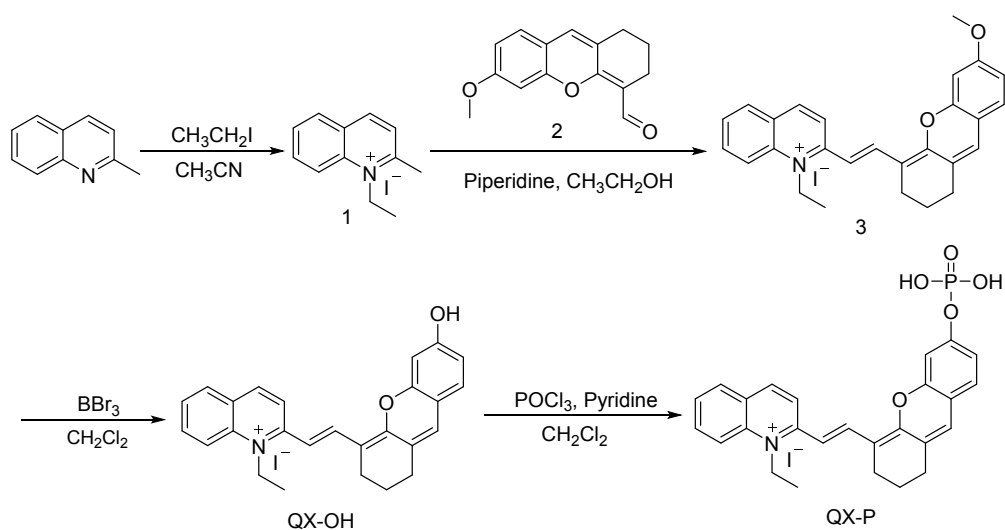
where σ is the standard deviation of the emission intensity of QX-P and k is the slope between the emission intensity and concentration.

Cell incubation and fluorescence imaging. HepG2 (human hepatoma cells), HeLa (human cervix cancer cells), HCT116 (human colon cancer cells), and 4T1 (breast cancer cells) were obtained from the State Key Laboratory of Chemo/Biosensing and Chemometrics of Hunan University (Changsha, China). The cells were cultured in DMEM (Dulbecco's modified Eagle's medium) containing 1% antibiotics (100 U/mL penicillin and 100 μ g/mL streptomycin) and 10 % FBS (fetal bovine serum) in an atmosphere of 37 °C and 5% CO₂. The cells were separated into three groups and treated with different condition. The first group of cells served as a control group without any treatment. The second group of cells were treated with the QX-P (10 μ M) at 37 °C for 30 min. The third group of cells were incubated with 100 μ M Na₃VO₄ at 37 °C for 30 min, then incubated with QX-P (10 μ M) for 30 min. All

the cells were washed by PBS buffer solution three times before imaging. Fluorescence imaging of the cells were performed by a confocal fluorescence microscope.

Fluorescence imaging in mice. Male Kunming mice of 18-24 g in weight were purchased from Hunan Anshengmei Drug Research Institute Co. Ltd (Changsha, China), used and kindly kept in all the experimental process. All experiments were performed in accordance with “Regulations of Hunan province on the administration of experimental animals”, and approved by the ethics committee at Hunan Anshengmei Drug Research Institute Co. Ltd. All mice were divided into three groups and treated differently. The first group was normal group, which were intraperitoneally injected with 100 μ L saline solution once daily for 7 days. The second group was diabetes group, which were injected intraperitoneally streptozotocin (STZ) dissolved freshly in 0.01 M citrate buffer (pH 4.5) at a dose of 150 mg/kg body weight (BW). After three days, the blood glucose levels of mice were greater than 16.7 mmol/L, which showed that the diabetic mice model was successfully established. The third group was treatment group, which was the therapy of the diabetic mice with oral gavage of 100 μ L metformin (Metf) saline solution (200 mg/kg BW) for 7 days. All mice were then injected intravenously with QX-P (100 μ L, 200 μ M), and imaged by small animal optical in vivo imaging system.

2. Synthesis of probes.



Scheme S1. Synthetic route for QX-P.

Compound 1. 2-methylquinoline (1.43 g, 10 mmol) and $\text{CH}_3\text{CH}_2\text{I}$ (2.32 g, 15 mmol) were dissolved in CH_3CN (20.0 mL). The mixture was refluxed for 16 h. Then the reaction solution was poured into ice water, the crude product was filtered and washed with ether to obtain a light yellow powder. Yield: 2.24 g (75%). $^1\text{H NMR}$ (400 MHz, DMSO) δ 9.12 (d, $J = 8.4$ Hz, 1H), 8.61 (d, $J = 8.6$ Hz, 1H), 8.46-8.43 (m, 1H), 8.24-8.20 (m, 1H), 8.13 (d, $J = 8.5$ Hz, 1H), 7.99 (t, $J = 7.8$ Hz, 1H), 4.99 (q, $J = 7.28$ Hz, 2H), 3.13 (s, 3H), 1.51 (t, $J = 7.5$ Hz, 3H); MS (TOF): 172.3.

Compound 3. Compound 2 was synthesized according to the reference (Sens Actuators B Chem., 2020, 320, 128296). Compound 1 (0.17 g, 1.0 mmol) and compound 2 (0.25 g, 1.2 mmol) was dissolved in EtOH (10 mL). Next, piperidine (0.3 mL) was added under stirring condition, the mixture was refluxed for 16 h. The solid obtained after concentration is purified by column chromatography ($\text{CH}_2\text{Cl}_2:\text{CH}_3\text{OH} = 30:1$) to obtain a blue solid. Yield: 0.33 g (64%). $^1\text{H NMR}$ (400 MHz, DMSO) δ 8.75 (d, $J = 8.8$ Hz, 1H), 8.65-8.57 (m, 2H), 8.40 (d, $J = 8.9$ Hz, 1H), 8.23-8.17 (m, 1H), 8.05 (t, $J = 7.9$ Hz, 1H), 7.81 (t, $J = 7.7$ Hz, 1H), 7.40 (d, J

= 8.2 Hz, 1H), 7.15 (d, J = 2.5 Hz, 1H), 7.09 (s, 1H), 6.83 (d, J = 8.4 Hz, 1H), 6.72 (d, J = 14.2 Hz, 1H), 4.93 (q, J = 7.0 Hz, 2H), 3.84 (s, 3H), 2.69 (t, J = 7.3 Hz, 4H), 1.84-1.79 (m, 2H), 1.51 (t, J = 6.9 Hz, 3H); MS (TOF): 396.3.

Compound QX-OH. Compound 3 (0.22 g, 0.5 mmol) was dissolved in dry CH₂Cl₂ (8 mL), BBr₃ (2.53 g, 10.0 mmol) was dropped into the above solution at 0 °C. Then, the mixture was continued to stir for 16 h at room temperature. Next, the saturated NaHCO₃ solution was added to the above solution at 0 °C, and it was extracted with CH₂Cl₂/ CH₃OH (10:1, v/v). The collected organic layer was dried by anhydrous Na₂SO₄ and the solvent was removed. The obtained product was further purified by column chromatography (CH₂Cl₂:CH₃OH = 8:1) to obtain a dark blue solid. Yield: 0.18 g (72%). ¹H NMR (400 MHz, DMSO) δ 10.35 (s, 1H), 8.67 (d, J = 9.2 Hz, 1H), 8.57 (t, J = 11.1 Hz, 2H), 8.34 (d, J = 9.0 Hz, 1H), 8.22 (d, J = 7.8 Hz, 1H), 8.03 (t, J = 8.0 Hz, 1H), 7.78 (t, J = 7.5 Hz, 1H), 7.25 (d, J = 8.4 Hz, 1H), 7.07 (s, 1H), 6.92 (s, 1H), 6.72-6.66 (m, 2H), 4.91 (q, J = 6.8 Hz 2H), 2.63 (t, J = 7.1 Hz, 4H), 1.84-1.79 (m, 2H), 1.52 (t, J = 7.1 Hz, 3H); ¹³C NMR (100 MHz, DMSO) δ 160.7, 156.8, 154.3, 142.2, 141.7, 138.7, 134.7, 130.5, 129.5, 128.6, 128.1, 127.3, 126.2, 121.0, 118.6, 114.3, 113.2, 112.3, 102.8, 45.7, 29.1, 24.8, 20.7, 13.8; MS (TOF): 382.3.

Compound QX-P. QX-OH (76.4 mg, 0.2 mmol) and pyridine (0.3 mL) was dissolved in dry CH₂Cl₂ (5 mL), and phosphorus oxychloride (0.2 mL) was slowly added to the above solution at 0 °C. After stirring for 4 h at room temperature, the ice water (5 mL) was poured into the resulting mixture and stirred overnight. After the solvent was concentrated, the obtained product was purified by column chromatography (CH₂Cl₂:CH₃OH = 2:1) to afford a dark purple solid. Yield: 69.4 mg (59%). ¹H NMR (400 MHz, DMSO) δ 8.46-8.36 (m, 3H),

8.16 (d, J = 8.6 Hz, 1H), 8.08 (d, J = 7.8 Hz, 1H), 7.92 (t, J = 7.7 Hz, 1H), 7.66 (t, J = 7.5 Hz, 1H), 7.23 (d, J = 8.6 Hz, 1H), 7.14 (s, 1H), 6.79 (s, 1H), 6.60 (d, J = 10.2 Hz, 1H), 6.49 (d, J = 14.3 Hz, 1H), 4.76 (q, J = 6.4 Hz, 2H), 2.62 (t, J = 5.5 Hz, 4H), 1.81-1.75 (m, 2H), 1.47 (t, J = 7.0 Hz, 3H). ¹³C NMR (100 MHz, DMSO) δ 157.4, 155.2, 153.5, 140.4, 139.9, 138.9, 134.1, 131.5, 130.2, 128.9, 127.2, 126.7, 124.0, 120.9, 117.8, 114.2, 112.7, 108.4, 103.0, 45.0, 28.8, 24.8, 20.9, 13.4; MS (TOF): 462.2. Elem. anal. (%) calcd. for C₂₆H₂₅INO₅P: C, 52.99, H, 4.28, N, 2.38. Found: C, 53.01, H, 4.26, N, 2.37.

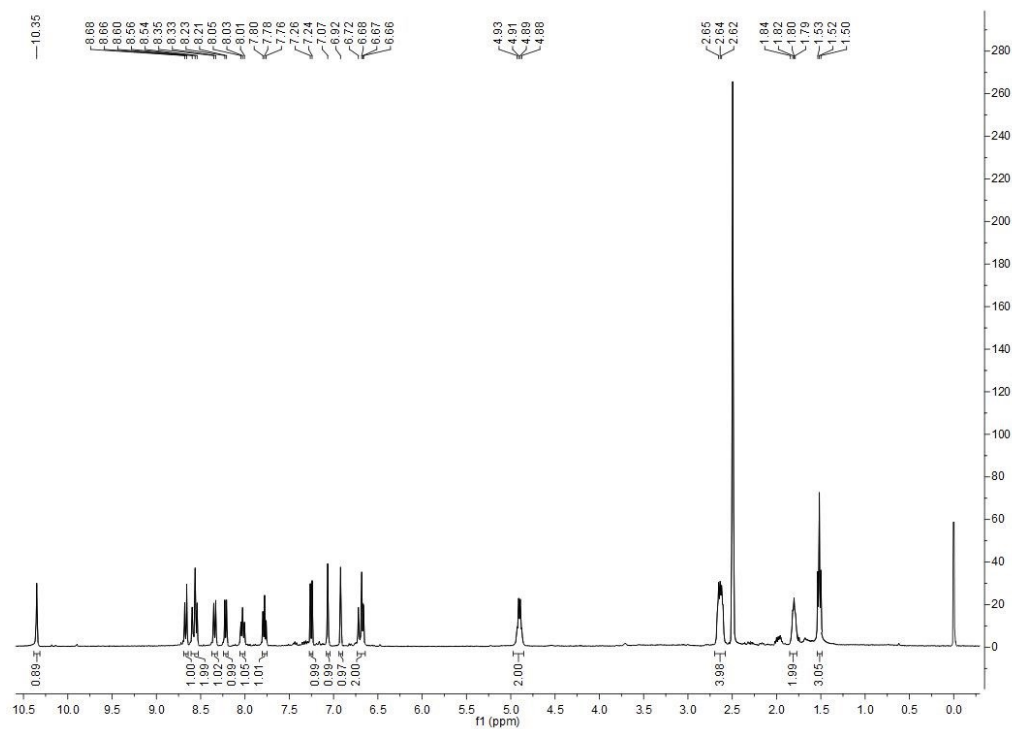


Fig. S1. ^1H NMR spectra of compound QX-OH in DMSO-d_6

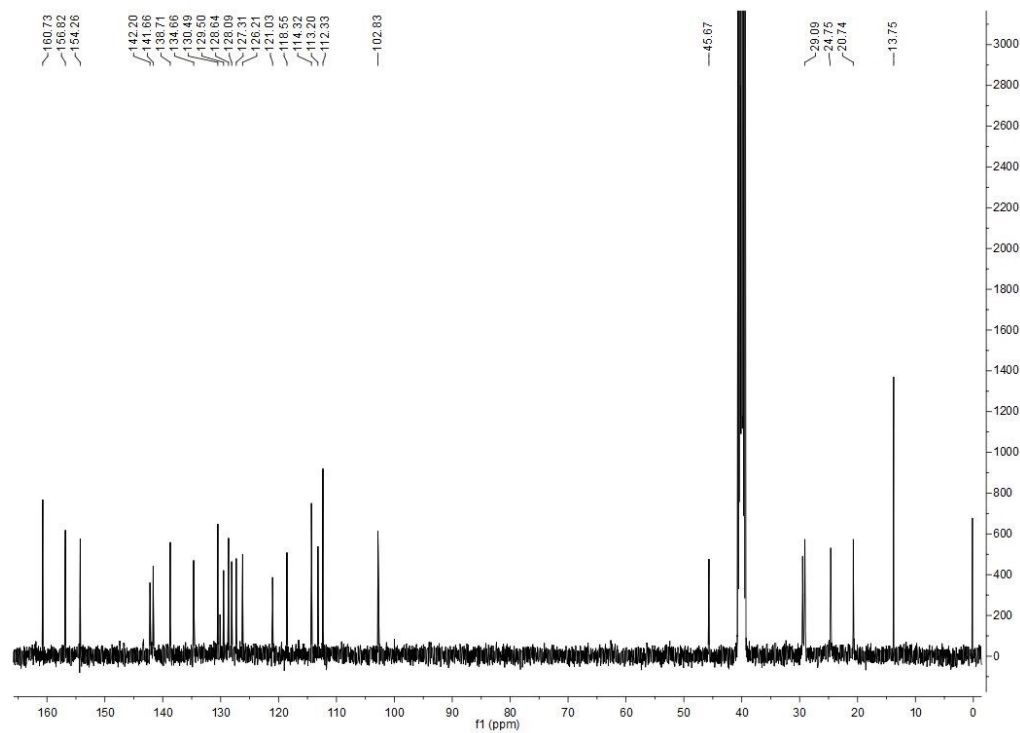


Fig. S2. ^{13}C NMR spectra of compound QX-OH in DMSO-d_6 .

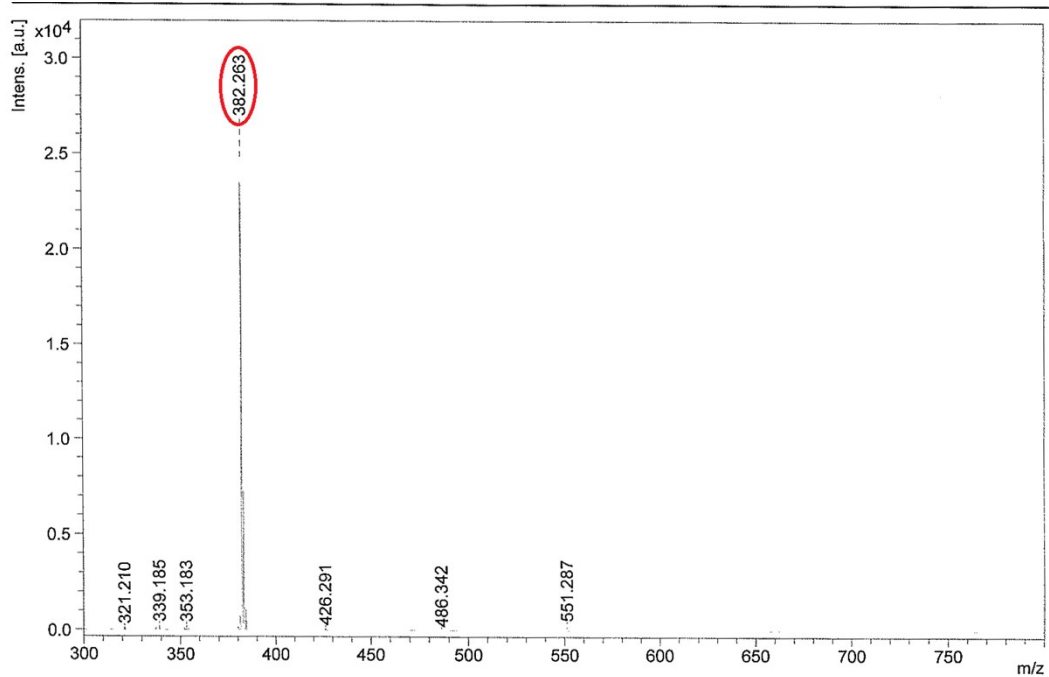


Fig. S3. Mass spectra of compound QX-OH.

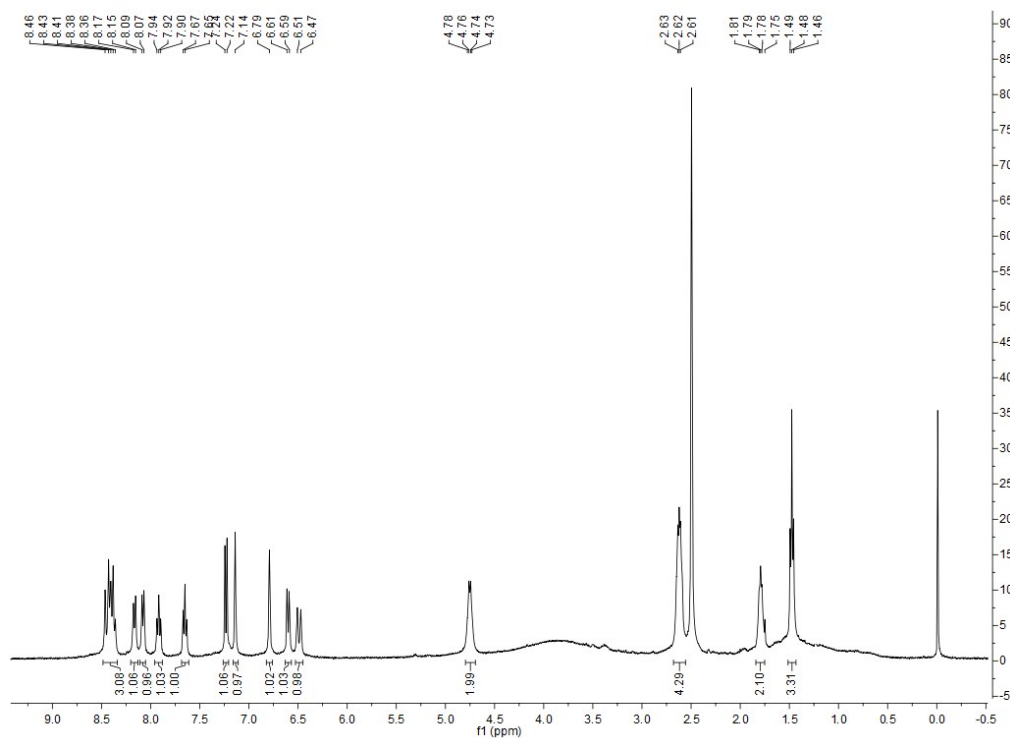


Fig. S4. ¹H NMR spectra of compound QX-P in DMSO-d₆.

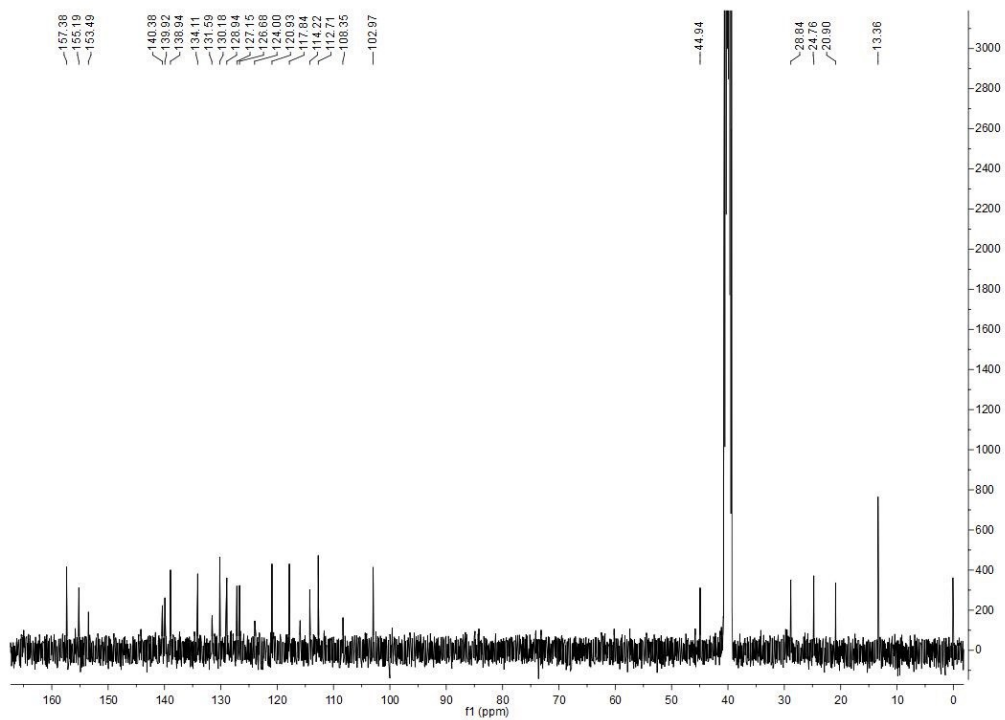


Fig. S5. ^{13}C NMR spectra of compound QX-P in DMSO-d_6 .

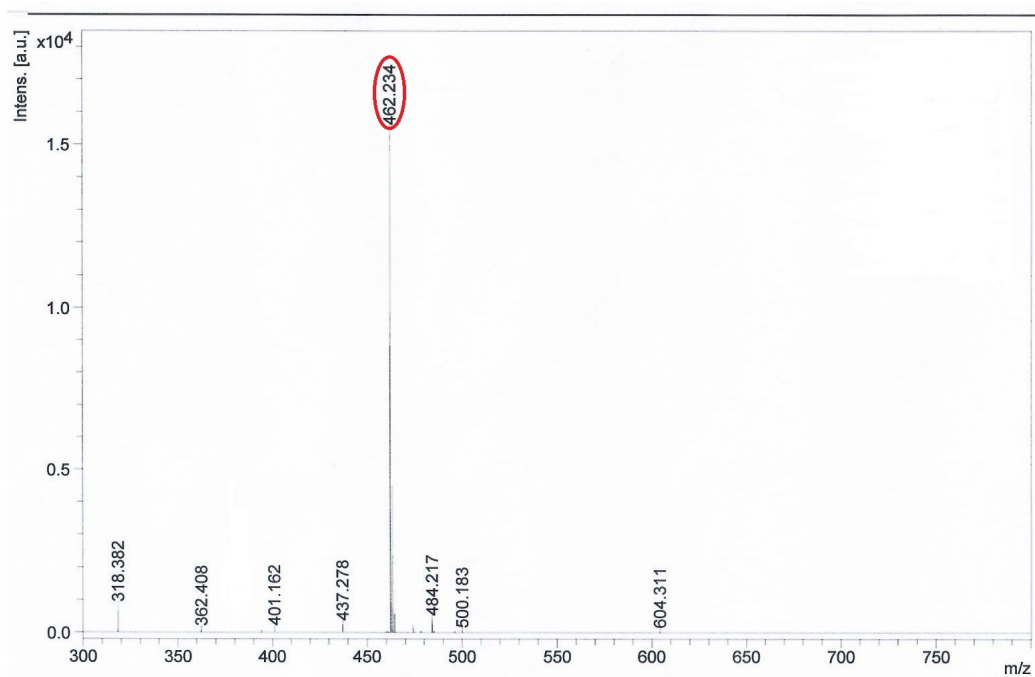


Fig. S6. Mass spectra of compound QX-P.

3. Spectral data.

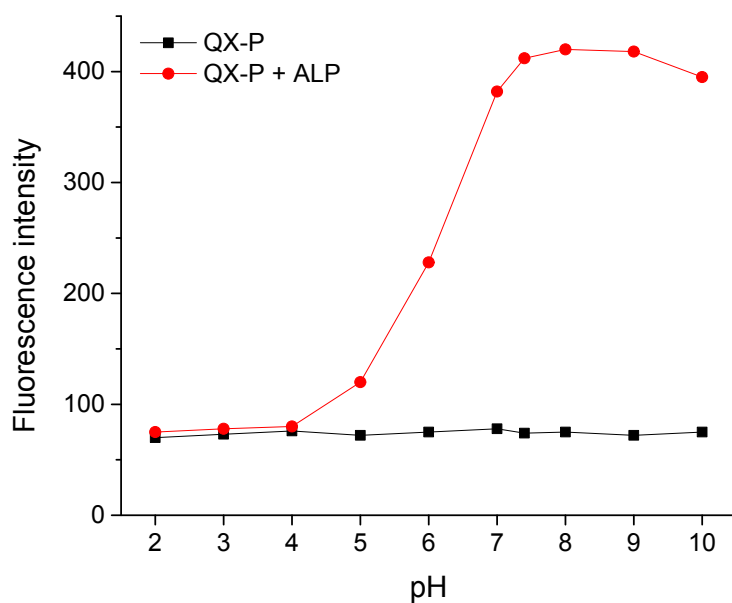


Fig. S7. Effect of pH on the fluorescence of QX-P (10 μ M) before and after reaction with ALP (1.0U/mL). $\lambda_{\text{ex}} = 720$ nm.

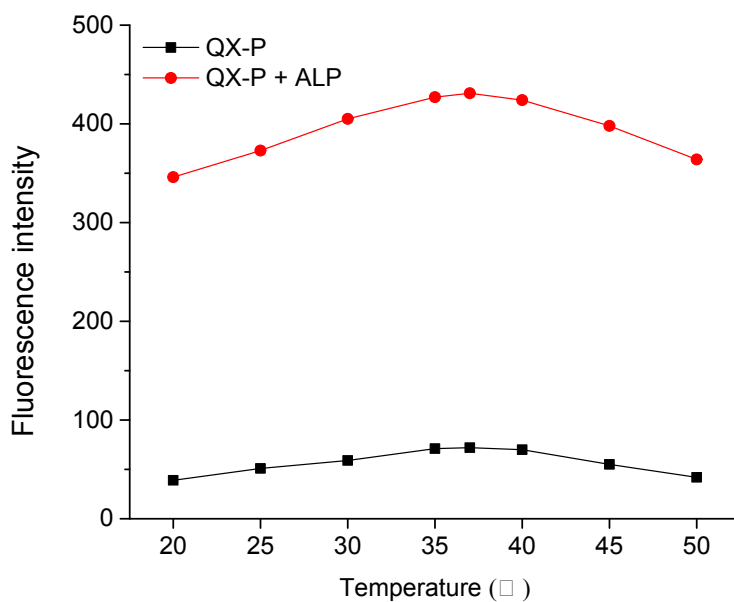


Fig. S8. Effect of temperature on the fluorescence of QX-P (10 μ M) before and after reaction with ALP (1.0 U/mL) in Tris-HCl buffer solution (pH 8.0, 50 mM). $\lambda_{\text{ex}} = 720$ nm.

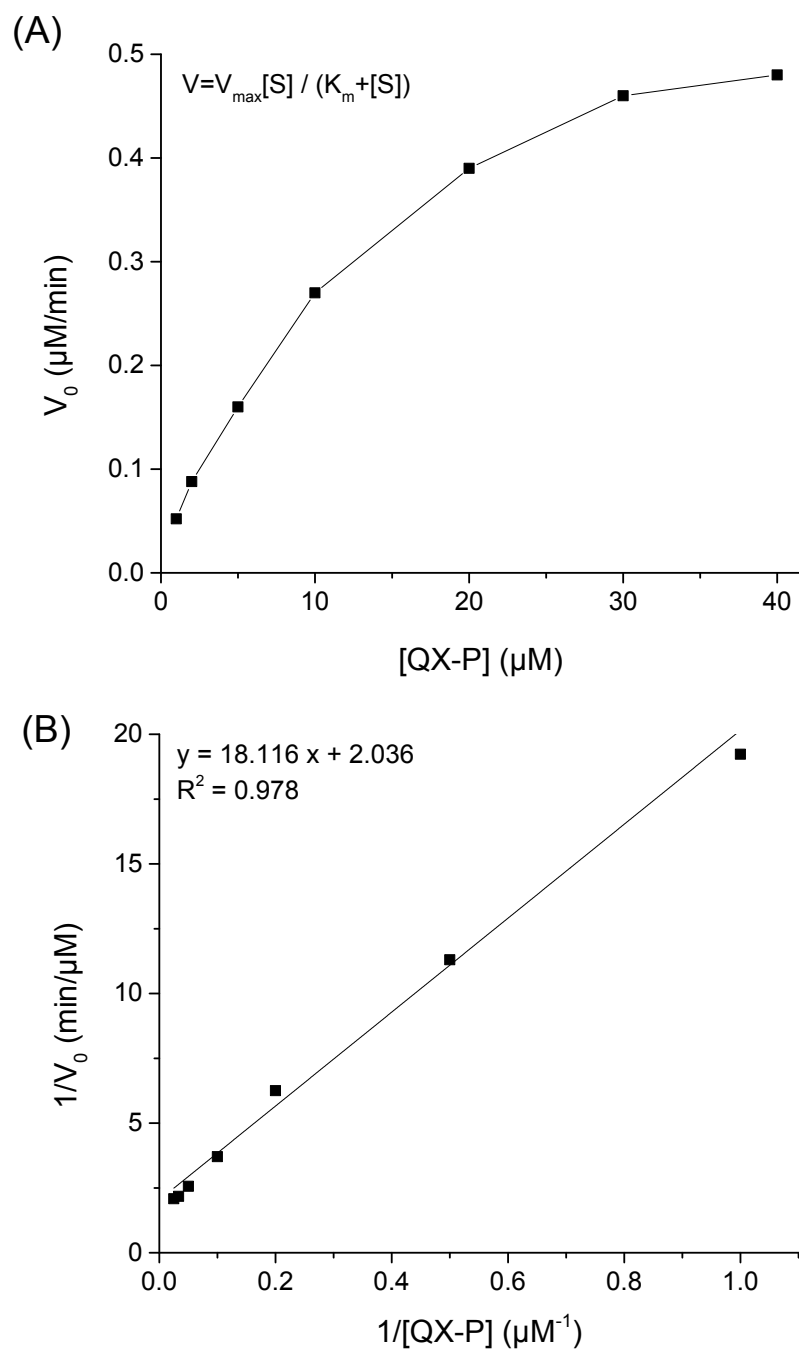


Fig. S9. (A) Michaelis-Menten plot and (B) Lineweaver-Burke plot for the reaction between QX-P and ALP (1.0 U/mL) in Tris-HCl buffer solution (50 mM, pH 8.0).

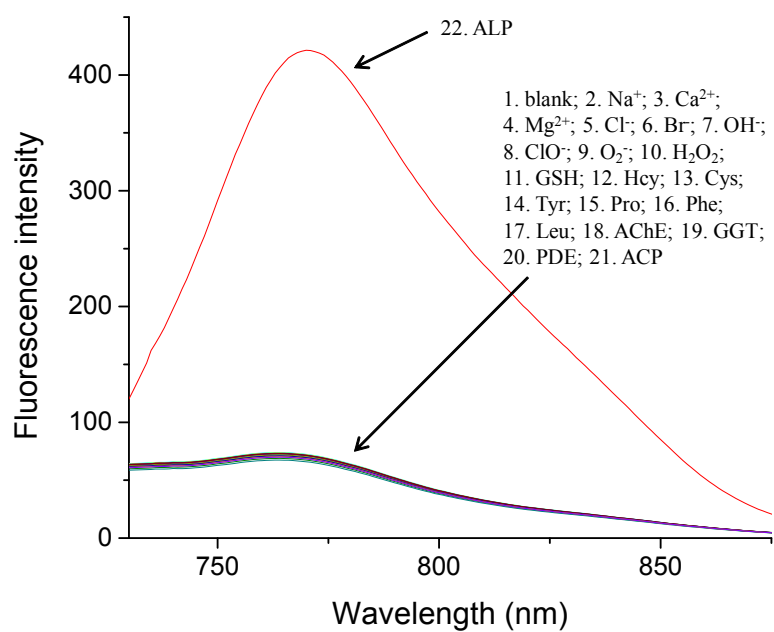


Fig. S10. Fluorescence spectra of QX-P (10 μ M) to various analytes in Tris-HCl buffer solution (pH 8.0, 50 mM). $\lambda_{\text{ex}} = 720$ nm.

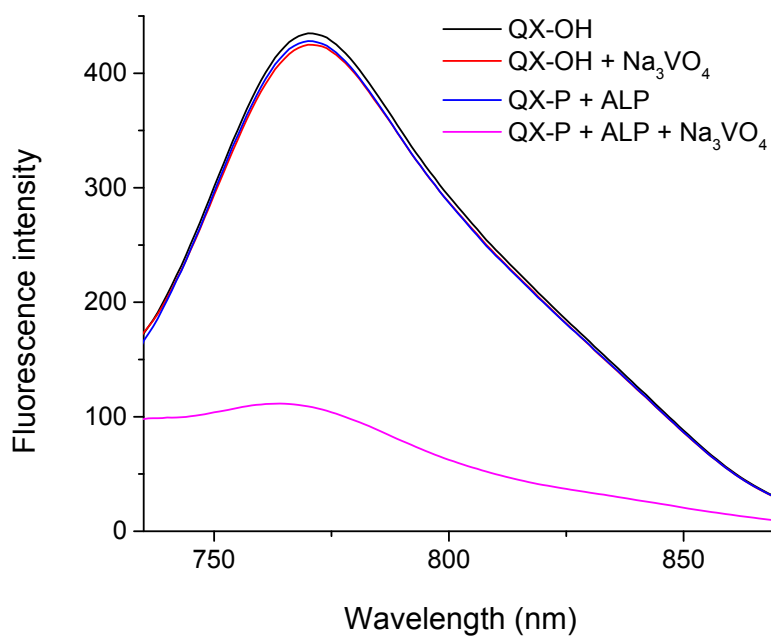


Fig. S11. Effect of inhibitor (Na_3VO_4) on the fluorescence of QX-OH. $\lambda_{\text{ex}} = 720$ nm.

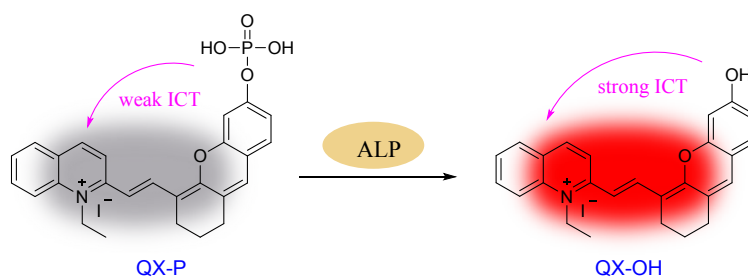
4. Response mechanism.

A possible reaction mechanism of QX-P to ALP was come forward in Scheme S2. The phosphate moiety of QX-P is catalytically cleaved by ALP to induce the transformation of QX-P into QX-OH. QX-P itself is no fluorescent due to the hydroxyl group of QX-OH is replaced by phosphate moiety, which hinders the ICT process. When ALP is added, the phosphate moiety of QX-P is hydrolyzed and the hydroxyl group is released, causing the ICT process to resume and a strong fluorescent signal appears.

To certify the above response mechanism, HPLC analysis was performed and the results were given in Fig. S12. QX-P itself shows a major peak at 3.2 min. After reacted with ALP, it was observed that the signal peak at 3.2 min disappeared, and a new signal peak appeared at 11.3 min (the same retention time with QX-OH). Furthermore, MS analysis was also studied. For free QX-P, the peak was at $m/z = 462.5$. After adding ALP, the peak at $m/z = 462.5$ reduced and a main new peak at $m/z = 382.4$ corresponding to QX-OH appeared (Fig. S13). It can be seen from the above results that QX-P can be cleaved efficiently by ALP and accompanied by the generation of QX-OH.

Moreover, in order to understand deeply the reaction mechanism of QX-P to ALP, density functional theory (DFT) calculation by using Gaussian 09 package were carried out. The optimized structures of QX-P and QX-OH were shown in Fig. S14A. And the highest occupied molecular orbital (HOMO) and the lowest unoccupied molecular orbital (LUMO) of them are provided in Fig. S14B. QX-OH is composed of a donor and an acceptor, making the intramolecular ICT process constitutes a push-pull system, which causes the fluorescence to turn on. On the contrary, the phosphate moiety in QX-P acts as an electron withdrawing group

to block the ICT process, causing the fluorescence to turn off. The HOMO-LUMO energy gaps of QX-P and QX-OH are calculated to be 2.11 and 2.09 eV, respectively. The theoretical calculation is consistent with the experimental results, verifying the proposed response mechanism.



Scheme S2. Proposed reaction mechanism for QX-P and ALP.

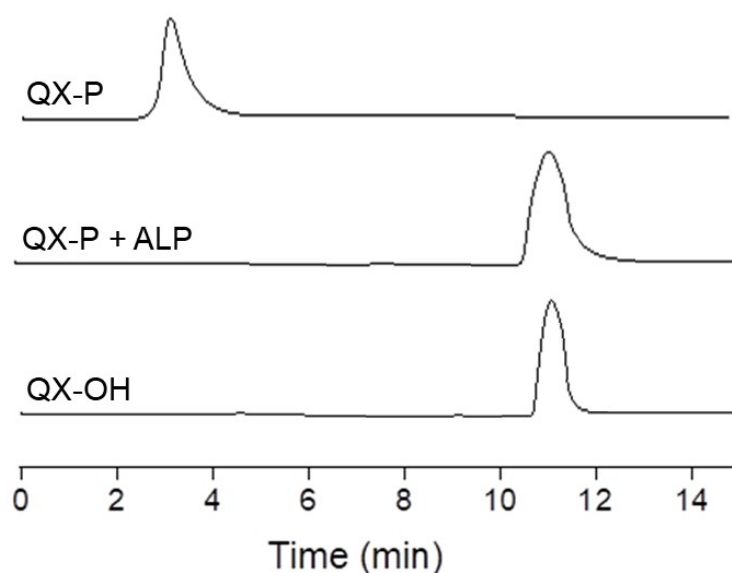


Fig. S12. HPLC chromatograms of QX-P, QX-P reacted with ALP, and QX-OH. HPLC mobile phase: methanol/H₂O = 90/10 (v/v).

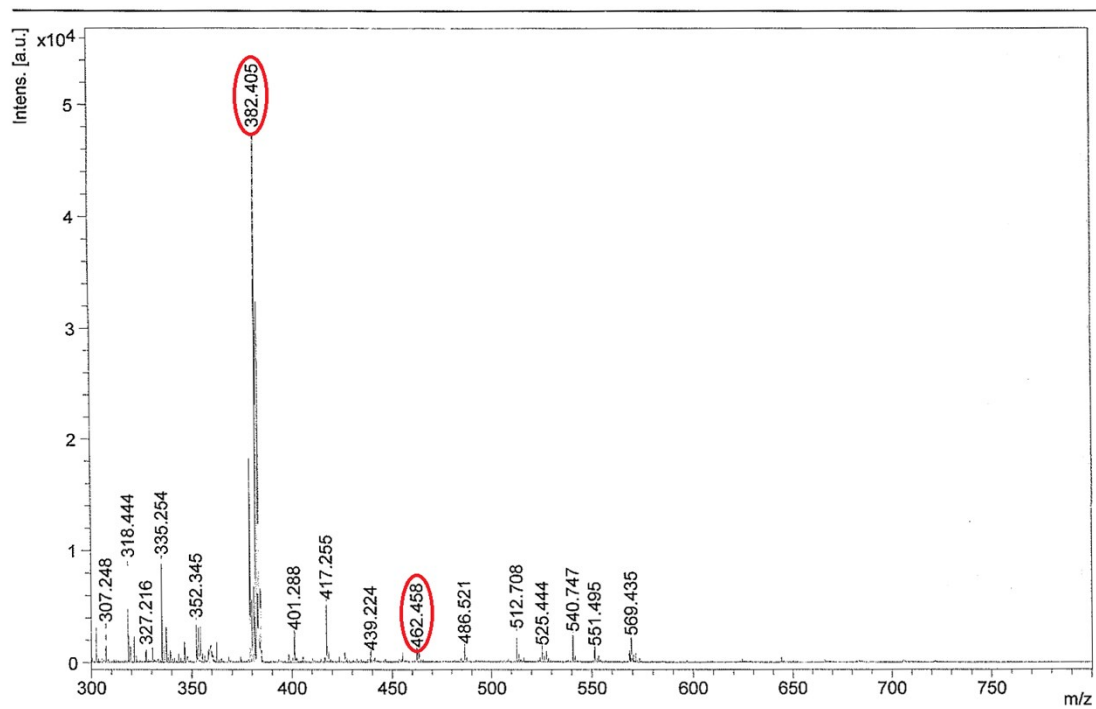


Fig. S13. Mass spectra of QX-P reacted with ALP.

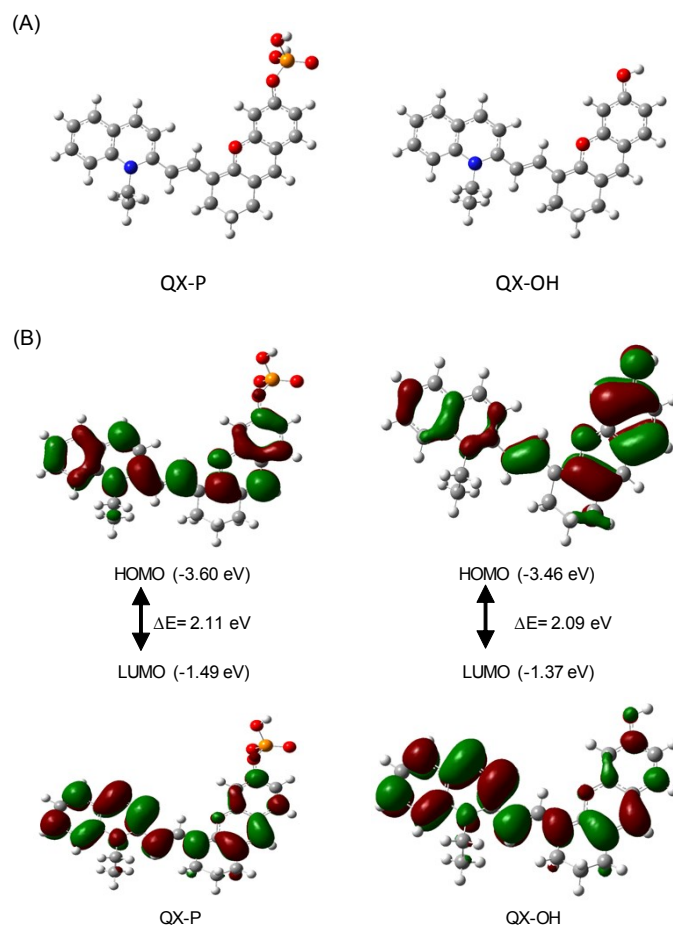


Fig. S14. (A) The optimized structures of QX-P and QX-OH. In the ball-and-stick model, carbon, oxygen and nitrogen atoms are colored in gray, red and blue, respectively. (B) Frontier molecular orbitals of QX-P and QX-OH.

5. Biological assays.

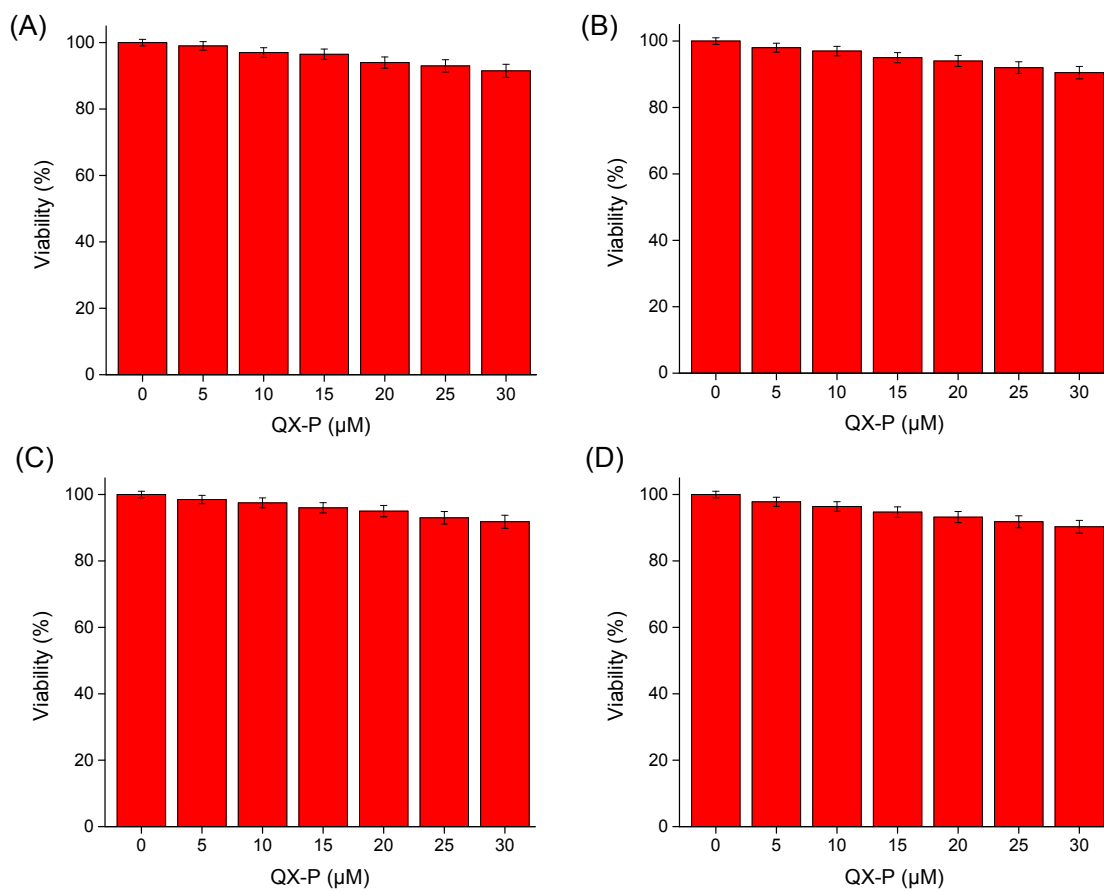


Fig. S15. MTT assay for estimating cell viability (%) of (A) HeLa cells, (B) HepG2 cells, (C) HCT116 cells and (D) 4T1 cells treated with various concentrations of QX-P (0-30 μM) after 24 h incubation.

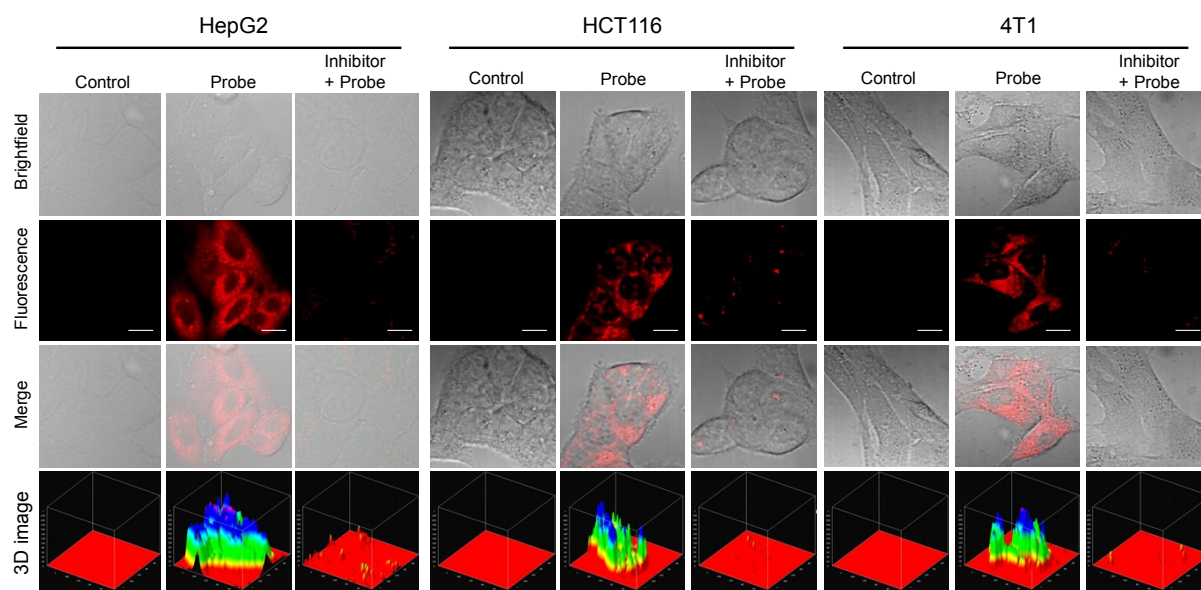


Fig. S16. Fluorescence images of HepG2, HCT116 and 4T1 cells. Control group: the cells were untreated with QX-P; probe group: the cells treated with QX-P only; inhibitor + probe group: the cells treated with Na_3VO_4 and QX-P. $\lambda_{\text{ex}} = 640 \text{ nm}$, $\lambda_{\text{em}} = 700\text{-}775 \text{ nm}$. Scale bar: $10 \mu\text{m}$.

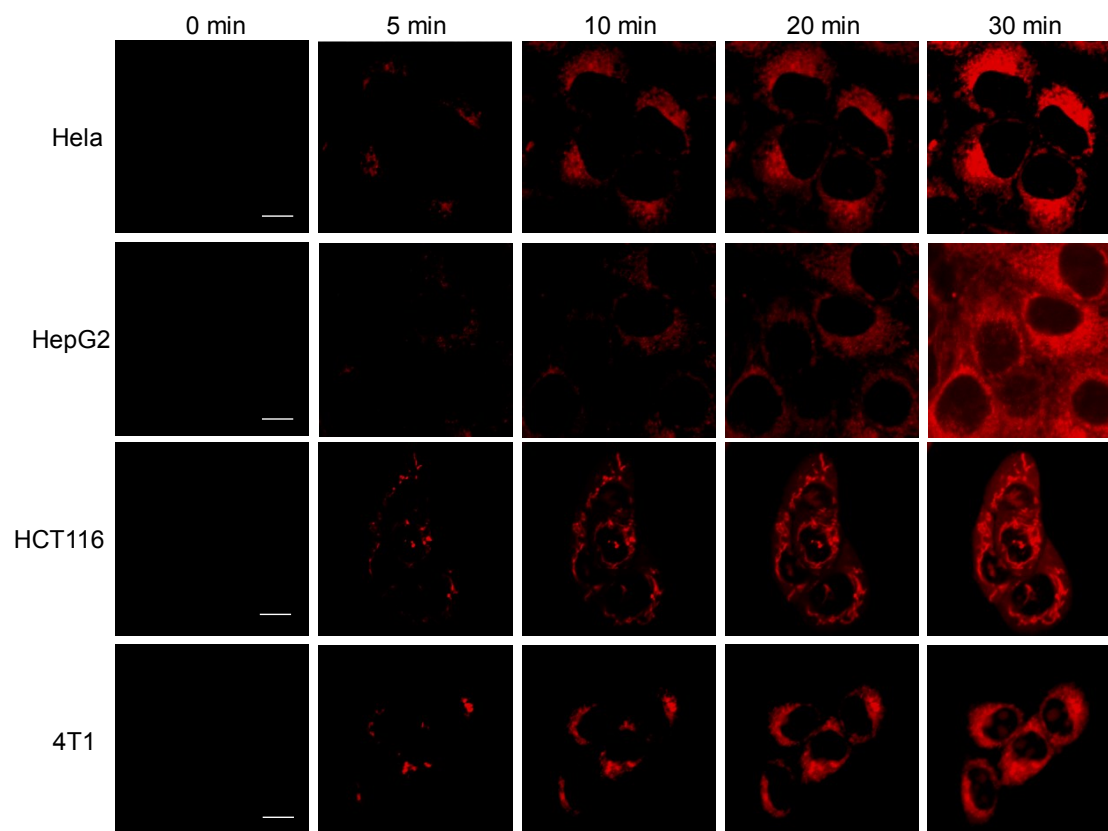


Fig. S17. The time-dependent fluorescence response of QX-P to ALP activity in Hela, HepG2, HCT116 and 4T1 cells. The cells were incubated with QX-P (10 μ M) at different time points: 0, 5, 10, 20 and 30 min. $\lambda_{\text{ex}} = 640$ nm, $\lambda_{\text{em}} = 700\text{-}775$ nm. Scale bar: 10 μ m.

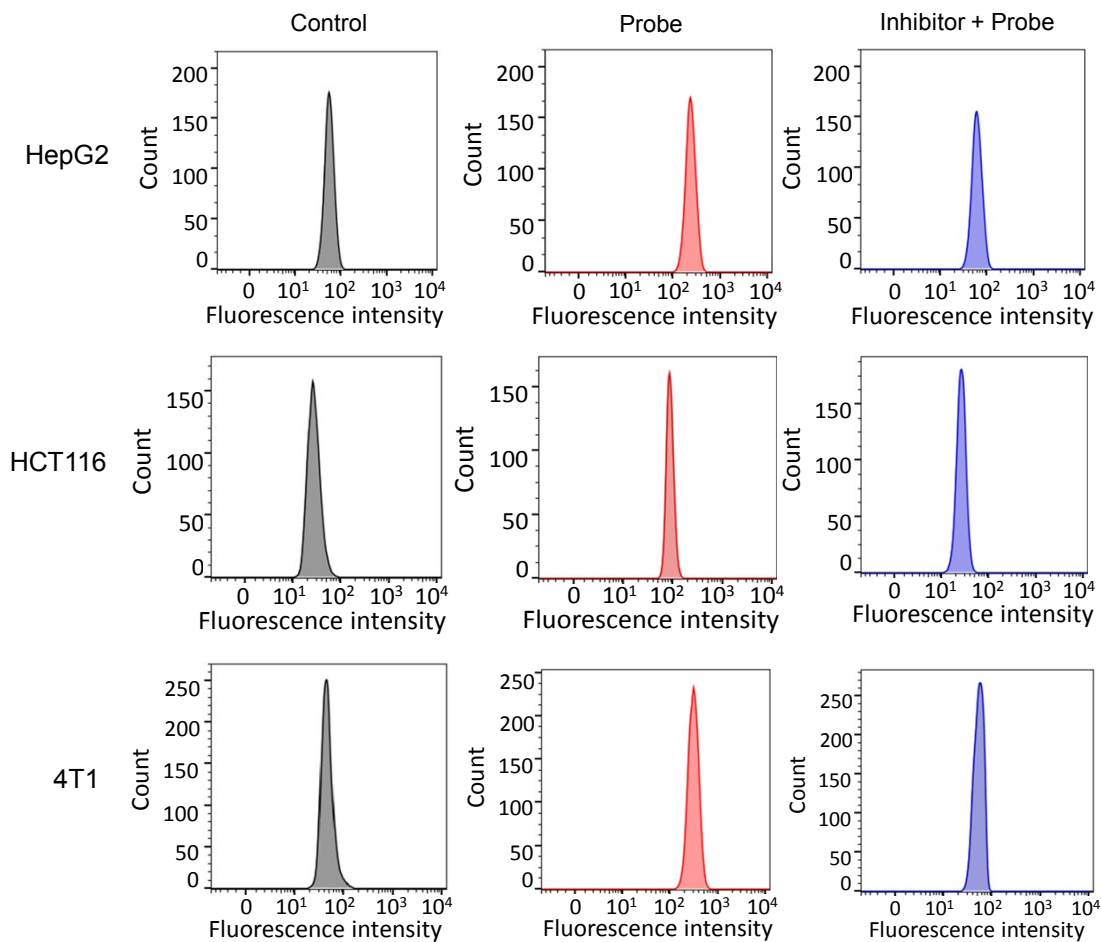


Fig. S18. Flow cytometry analysis. Control group: the cells were untreated with QX-P; probe group: the cells treated with QX-P only; inhibitor + probe group: the cells treated with Na_3VO_4 and QX-P.